Zitierweise: *Angew. Chem. Int. Ed.* **2021**, *60*, 13952–13958
Internationale Ausgabe: doi.org/10.1002/anie.202016393
Deutsche Ausgabe: doi.org/10.1002/ange.202016393

VIP **Polymerization** *Very Important Paper*

# An Ion-Pairing Approach to Stereoselective Metal-Free Ring-Opening Metathesis Polymerization

*Xuejin Yang[+], Sean R. Gitter[+], Allison G. Roessler[+], Paul M. Zimmerman* and Andrew J. Boydston**

***Abstract:*** *Stereochemistry can have a profound impact on polymer and materials properties. Unfortunately, straightforward methods for realizing high levels of stereocontrolled polymerizations are often challenging to achieve. In a departure from traditional metal-mediated ring-opening metathesis polymerization (ROMP), we discovered a remarkably simple method for controlling alkene stereochemistry in photoredox mediated metal-free ROMP. Ion-pairing, initiator sterics, and solvation effects each had profound impact on the stereochemistry of polynorbornene (PNB). Simple modifications to the reaction conditions produced PNB with trans alkene content of 25 to >98%. High cis content was obtained from relatively larger counterions, toluene as solvent, low temperatures (−78°C), and initiators with low Charton values. Conversely, smaller counterions, dichloromethane as solvent, and enol ethers with higher Charton values enabled production of PNB with high trans content. Data from a combined experimental and computational investigation are consistent with the stereocontrolling step of the radical cationic mechanism proceeding under thermodynamic control.*

## Introduction

Ring-opening metathesis polymerization (ROMP) is used to make important commodity polymers such as polynorbornene (PNB), polydicyclopentadiene, and polycyclooctadiene among others.[1,2] Importantly, the unsaturation of these monomers is conserved during the polymerization, resulting in a polymer backbone that is rich in 1,2-disubstituted alkenes. The microstructures of polymer made by norbornene based monomers, in particular the double-bond geometries (*trans* versus *cis*), tacticities, and regioselectivity have each shown a strong relationship with polymer physical and mechanical properties.[3–8] For example, the glass transition temperature ($T_g$) of PNB increases with *cis* alkene content. Further, crystalline syndiotactic *cis*-PNB displays a high melting point ($T_m$), whereas amorphous atactic *trans*-PNB exhibits a wide softening range that is generally at lower temperatures.[9,10] Therefore, from an applications-oriented perspective, it is desirable to precisely control the stereochemistry of ROMP products.

Advances in stereocontrolled ROMP have unsurprisingly centered on the reactivities of metal-alkylidenes. Although there are notable examples of stereocontrol in ROMP from readily accessible metal initiator systems, targeted alkene stereoselectivity has generally required specially engineered metal initiators. In some cases, the new designs compromise desirable attributes of more general initiators, such as breadth of monomer scope, functional group tolerance, stability, and overall activity. Additionally, there are not straightforward approaches to modify a highly *trans*-selective metal catalyst to make it highly *cis*-selective (nor vice versa), or to otherwise tailor stereoselectivities with high precision. Important successes with stereoselective ROMP have been achieved by using well-defined Mo-, W-, and Ru-based alkylidene initiators,[9,11–21] or employing functionalized monomers that induce stereoregular polymerization with metal-alkylidene initiators.[22,23] Custom organometallic initiators are designed with ligands that impose facial selectivity of the incoming monomer to the metal-alkylidene chain end to favor either a *cis* or *trans* metallacyclobutane. In this general mechanistic approach, the metallacyclobutane stereochemistry determines the alkene geometry following [2+2] cycloelimination (Scheme 1). Another technique uses a Grubbs 2nd generation catalyst with cyclopropene based monomers to generate exclusively *trans* alkene polymers by cleaving *cis* „errors" with a rapid ring-closing metathesis reaction.[24]

Metal-free ROMP (MF-ROMP) presents fundamentally unique mechanistic features compared to essentially all other approaches to metathesis polymerization. Considering the significant change in reactivity landscape, we questioned how one might accomplish stereocontrol absent a metal-alkylidene. Photoredox mediated MF-ROMP proceeds via single electron oxidation of enol ether initiators with pyrylium photooxidants, ultimately generating radical cationic chain ends that are reversibly deactivated (Scheme 2).[25,26] In our attempts to increase the solubility of pyrylium photocatalysts,

[*] Dr. X. Yang,[+] S. R. Gitter,[+] Prof. Dr. A. J. Boydston
Department of Chemistry, University of Wisconsin-Madison
Madison, WI 53706 (USA)
E-Mail: aboydston@wisc.edu
Prof. Dr. A. G. Roessler,[+] Prof. Dr. P. M. Zimmerman
Department of Chemistry, University of Michigan
Ann Arbor, MI 48109 (USA)
E-Mail: paulzim@umich.edu
Prof. Dr. A. G. Roessler[+]
Department of Chemistry, Oglethorpe University
Atlanta, GA 30319 (USA)
Prof. Dr. A. J. Boydston
Department of Chemical and Biological Engineering, Department of Materials Science and Engineering, University of Wisconsin-Madison
Madison, WI 53706 (USA)
[+] These authors contributed equally to this work.
Supporting information and the ORCID identification number(s) for the author(s) of this article can be found under: https://doi.org/10.1002/anie.202016393.

  

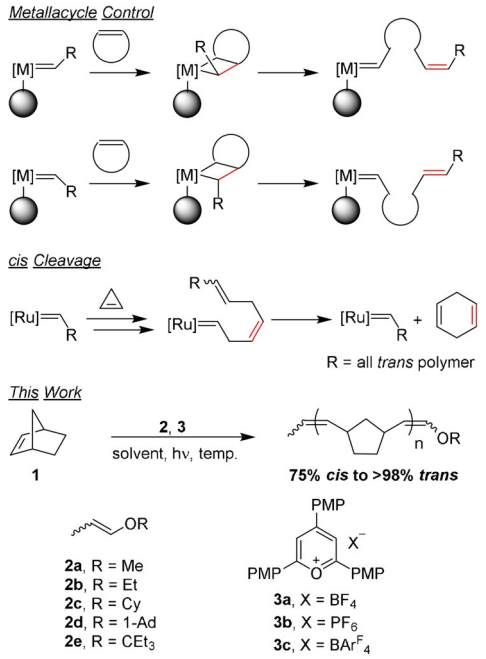


***Scheme 1.*** Summary of Approaches Toward Stereoselectivity During Metal-Mediated versus Metal-Free ROMP. PMP = *p*-methoxyphenyl.

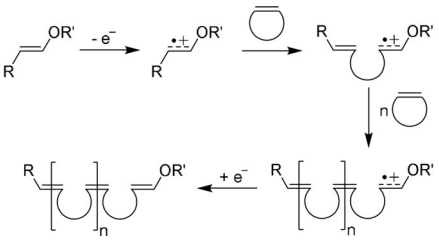


***Scheme 2.*** Abbreviated mechanism of MF-ROMP.

we observed that changes in the counteranion yielded different alkene *cis*/*trans* ratios in PNB. Moreover, access to a broader range of solvents revealed additional influences of ion pairing as well as temperature effects. Herein, we report on our discovery, experimental development, and computational understanding of stereoselectivity in MF-ROMP. This new platform provides a straightforward and easily tunable approach to control alkene geometry in ROMP products.

## Results and Discussion

Within the context of the MF-ROMP mechanistic hypothesis, we predicted that understanding the environment near the active chain end would reveal methods for controlling alkene stereoselectivity. Toward this end (Scheme 1, bottom), we investigated: (1) counteranions, which were influential in previously reported examples with poly(vinyl ethers) and asymmetric small molecule syntheses;[27–32] (2) reaction conditions, with emphasis on solvent and temperature; and (3) steric parameters of enol ether initiators. Typical conditions for MF-ROMP of norbornene use ethyl propenyl ether (**2b**) as initiator, 2,4,6-tris(4-methoxyphenyl)pyrylium tetrafluoroborate (**3a**) as photocatalyst, dichloromethane as solvent, and an LED light source with an emission centered at 450 nm, all at room temperature.

Our motivations to move away from dichloromethane, toward less hazardous solvents as well as bulk polymerizations, first led us to consider different counteranions of the pyrylium salts to augment solubility. To quickly screen the influence of counteranions, we first added several phase-transfer catalysts (PTCs),[33–35] as shown in Table S1, into the MF-ROMP reaction mixture. It was found that polymerizations containing PTCs with non-coordinating anions, such as tetrafluoroborate ($BF_4^-$), hexafluorophosphate ($PF_6^-$), and tetrakis(3,5-bis(trifluoromethyl)phenyl)borate ($BAr^F{}_4^-$), each yielded PNB in high conversion. Conversely, addition of PTCs with more strongly coordinating anions like chloride, bromide, and nitrate, which are usually more nucleophilic,[36] failed to yield any detectable amount of PNB. Nucleophilic attack by anions on the pyrylium cation or radical cationic intermediates likely precluded polymerization in these latter cases.

Interestingly, we observed that as the size of PTC anion increased from $BF_4^-$ to $PF_6^-$ to $BAr^F{}_4^-$, the *trans* alkene content of the polymer backbone decreased from 79% down to 58% (Table S1). Based on these promising results, we then synthesized discrete 2,4,6-tris(4-methoxyphenyl)pyryliums with $PF_6^-$ (**3b**) and $BAr^F{}_4^-$ (**3c**) counteranions. MF-ROMP under standard conditions using **3a–c** in dichloromethane each showed a similar *trans*/*cis* alkene ratio as observed during the corresponding PTC additive study (Table 1, entries 1–3; Figure 1a). Excitingly, the new pyrylium salt **3c**

***Tabelle 1:*** Results of MF-ROMP Under Various Conditions.

| entry | initiator | PC | solvent | temp [°C] | conversion [%][a] | $M_n$[b] | $M_w$[b] | $Đ$[b] | *trans*:*cis*[a] |
|---|---|---|---|---|---|---|---|---|---|
| 1 | **2b** | **3a** | $CH_2Cl_2$ | 22 | 86 | 15.5 | 22.0 | 1.4 | 79:21 |
| 2 | **2b** | **3b** | $CH_2Cl_2$ | 22 | 85 | 18.3 | 30.0 | 1.6 | 74:26 |
| 3 | **2b** | **3c** | $CH_2Cl_2$ | 22 | 77 | 15.6 | 22.5 | 1.4 | 56:44 |
| 4 | **2b** | **3c** | $CH_2Cl_2$ | −76 | 39 | 7.50 | 14.9 | 2.0 | 56:44 |
| 5 | **2b** | **3c** | toluene | 22 | 21 | 2.11 | 2.70 | 1.3 | 55:45 |
| 6 | **2b** | **3c** | toluene | −76 | 30 | 7.61 | 16.7 | 2.2 | 35:65 |
| 7 | **2a** | **3c** | toluene | −76 | 18 | 5.30 | 8.12 | 1.5 | 25:75 |
| 8[c,d] | **2a** | **3a** | $CH_2Cl_2$ | 25 | 38 | 5.43 | 8.28 | 1.5 | 70:30 |
| 9[c,d] | **2b** | **3a** | $CH_2Cl_2$ | 25 | 42 | 5.49 | 8.21 | 1.5 | 76:24 |
| 10[c,d] | **2c** | **3a** | $CH_2Cl_2$ | 25 | 42 | 6.16 | 8.45 | 1.4 | 83:17 |
| 11[c,d] | **2d** | **3a** | $CH_2Cl_2$ | 25 | 38 | 6.03 | 8.62 | 1.4 | 88:12 |
| 12[c,d] | **2e** | **3a** | $CH_2Cl_2$ | 25 | 35 | 5.10 | 6.90 | 1.4 | 92:8 |
| 13 | **2e** | **3a** | $CH_2Cl_2$ | −76 | 90 | 5.01 | 8.04 | 1.6 | >98:2 |
| 14[d] | **2e** | **3c** | $CH_2Cl_2$ | 25 | 40 | 14.6 | 30.1 | 2.2 | 90:10 |

[a] Determined using $^1$H NMR spectroscopy (see SI for details). [b] Determined by GPC analysis on crude reaction sample using multi-angle light scattering (MALS) and refractive index (RI) detection. Dispersity ($Đ$) = $M_w/M_n$. [c] Values for conversion, molecular weight data, and *trans*:*cis* ratios are each an average of three runs. [d] Polymerization intentionally stopped at ≈40% conversion, for internal comparison.

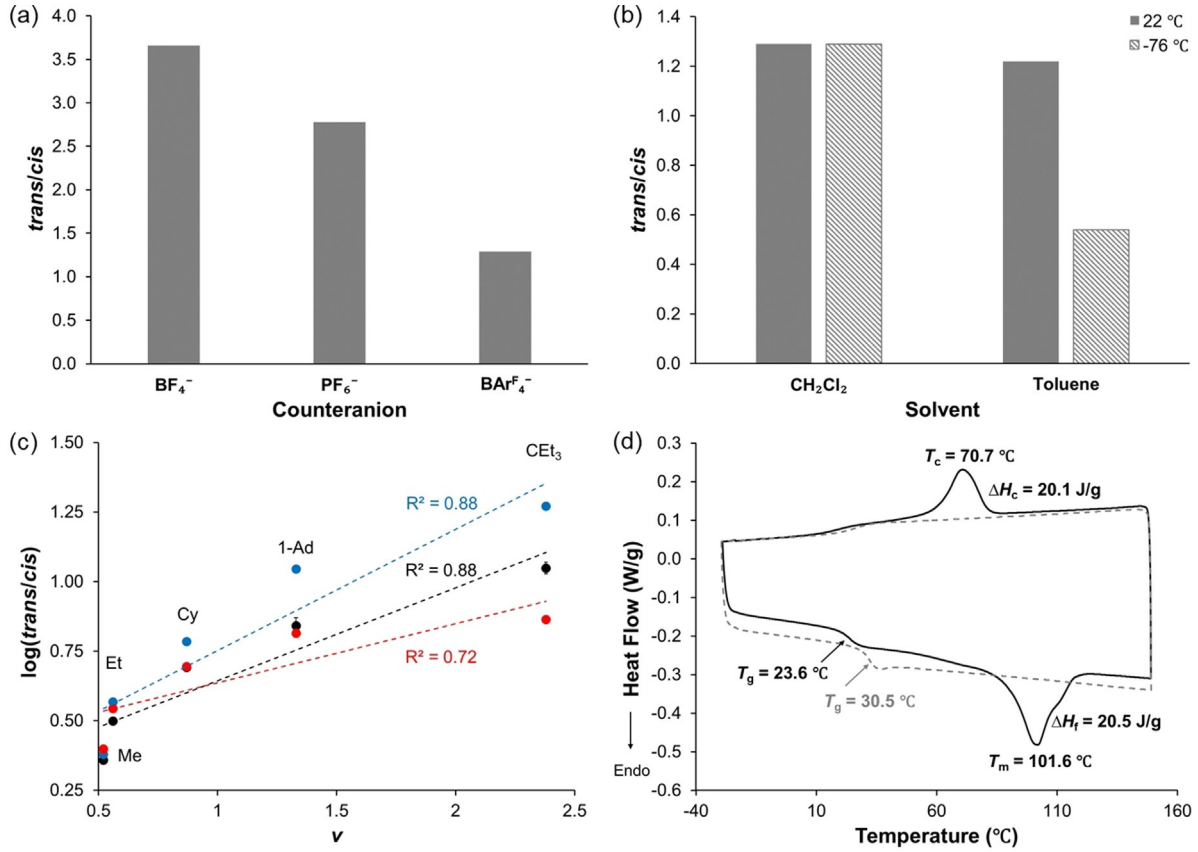


***Figure 1.*** Summary of a) counteranion effect (**2b**, $CH_2Cl_2$, 22 °C), b) solvent and temperature effects (**2b**, **3c**) on MF-ROMP stereoselectivity. c) Linear correlation of log(*trans*/*cis*) vs. Charton parameter ($\nu$) at −30 (blue), 25 (black), and 50 °C (red), slope = 0.44, 0.33 and 0.21, respectively. Points at 25 °C are the average of three runs. Error bars represent the standard deviation of the three runs. d) Representative DSC thermograms of PNB with > 98 % *trans* content (solid black line, Table 1, entry 13), and 75 % *cis* content (dashed gray line, Table 1, entry 7).

showed good solubility in both polar and nonpolar solvents, which was not observed with **3a** or **3b**.

Considering the importance of ion pairing in the observed stereocontrol, we next investigated solvent effects in MF-ROMP, aided by the improved solubility of **3c**. Using **3c** in toluene at room temperature gave a similar *trans*/*cis* alkene ratio as in dichloromethane (Table 1, entries 3 and 5), but with only ca. 20 % conversion of monomer. We ascribed the low conversion to rapid decomposition of **3c**, as indicated by loss of color and photoluminescence in the solution. We envisioned addition of polar solvents may help to stabilize the charge separated photocatalyst. Therefore, mixed solvent systems of toluene with various polar solvents were next investigated (Table S2). Solvent ratios for this study were chosen such that the nonpolar PNB remained visibly soluble throughout the polymerization. More polar solvent mixtures appeared to improve the stability of **3c**, as judged by the color of the reaction solution. We were surprised to find that more polar solvents also resulted in increased *trans* alkene content in the polymer, in contrast to the results using dichloromethane versus toluene. Solvents with high donicity,[37] like diethyl ether and acetone, were found to be detrimental to the polymerization. Using toluene/acetonitrile mixtures generally gave high conversions of monomer, and varying the pyrylium species (**3a**–**3c**) revealed that each pyrylium salt gave higher *trans*/*cis* ratios in toluene/acetonitrile mixture than in dichloromethane. Moreover, the *trans*/*cis* ratios decreased slightly with counteranion size (83:17, 82:18, and 82:18 for **3a**, **3b**, and **3c**, respectively). The results from counteranion and solvent screenings suggested to us that in weakly or noncoordinating solvents like dichloromethane and toluene, the affinity of the counteranion to the radical cationic chain end was dominant, as indicated by the greater differences in *trans*/*cis* ratio between anions in these solvents. The counteranion effects were reduced when the solvent polarity or donicity was increased, consistent with solvation competing more strongly with the anion.

Inspired by the general ability to modify stereoselectivity by controlling the environment around the radical cationic chain end, we next focused on initiator sterics as perhaps the most straightforward parameter to modulate alkene stereochemistry. Toward this end, we conducted a comparative analysis of initiators **2a**–**2e** which systematically increase the Charton parameter of the R group (Scheme 1). Each enol ether initiator was first evaluated using pyrylium **3a** as the photooxidant and dichloromethane as the solvent. Notably, we observed that as the steric bulk of the chain-end increased (higher Charton parameter), the *trans* alkene content of the polymer also increased (Table 1, entries 8–12). When we next applied each of the pyrylium salts (**3a**–**c**), we found that the

  

same counteranion effect was preserved across the initiator series. For example, we observed lower *trans* alkene content when **2e** was used with **3c** versus **3a** (Table 1, entry 14 cf. 12).

Temperature effects were initially less straightforward to interpret than those of counteranions or solvation. Moreover, our survey revealed that the influence of reaction temperature was codependent upon other reaction parameters, which was better understood through DFT calculations (vida infra). In general, stereoselectivities increased with decreasing temperature, although the magnitudes of the changes were dependent upon pyrylium counteranion and solvent. For example, use of **3c** in dichloromethane at 22 and −76 °C gave nearly identical *trans*/*cis* alkene ratios (Table 1, entries 3 and 4), whereas changing to toluene as solvent (entries 5 and 6) gave *trans*/*cis* ratios of 55:45 and 35:65 at 22 and −76 °C, respectively (see summary in Figure 1b). When **3a** was used as catalyst in combination with **2e** as initiator, the *trans*/*cis* alkene ratio changed from 92:8 to >98:2 when the temperature was changed from 25 to −76 °C (entries 12 and 13). Collectively, we learned that *trans* selectivity is favored by using large initiators, small counteranions, dichloromethane as solvent, and low temperatures, whereas *cis* selectivity is aided by small initiators, large counteranions, toluene as solvent, and low temperatures. Notably, through judicious choice of simple reaction parameters, we were able to modulate between 75 % *cis* alkene (Table 1, entry 7) to >98 % *trans* alkene (Table 1, entry 13) content in the polymer backbone, with the former showing amorphous structure while the latter exhibits semi-crystalline behavior as determined by differential scanning calorimetry (Figure 1d). Highly *trans* PNB showing semi-crystalline behavior is rarely reported.[9] A 2007 study indicated that PNB samples with *cis* content from 75–95 % showed melting transitions, however $M_n$ and tacticity (i.e., stereochemistry of the cycloalkane units) were not given.[10] We note that contributions to physicochemical properties from tacticity were not determined in this study.

We next focused on a deeper understanding of the mechanistic origins for the observed stereoselectivities. Linear free energy relationships (LFERs) are a powerful tool to investigate mechanistic influences of reactant substituents. With initiators **2a**–**2e** at hand, we investigated LFERs using Charton steric parameters as an approximation of the steric bulk of the initiator R group. Similar analyses have been used to quantify substituents' steric effects in enantioselective catalytic reactions as well as in a dynamic covalent reaction.[38,39] LFERs are generated by plotting the logarithm of the ratio of a reaction constant (e.g., rate or equilibrium constant) versus the parameter value. Using our data collected at 25 °C, the plot of $\log(trans/cis) = \psi\nu$, where $\psi$ is the slope of a linear fit and $\nu$ is a Charton value, gave an $R^2$ value of 0.88 (Figure 1c). In comparison, the plot of *trans*/*cis* vs. $\nu$ gave a linear fit having $R^2 = 0.99$ (Figure S2). Anslyn and co-workers reported a similar observation, greater linearity from the nonlogarithmic plot, when correlating the diastereomeric ratio (*dr*) to steric parameters for a thermodynamically controlled reaction.[39] Although, it is possible that the *trans*/*cis* ratio in our system shows better linearity versus Charton parameter than the plot using log(*trans*/*cis*) because of an imperfect correlation of Charton parameters with the enol ethers' steric bulk, we speculate that the stereodetermining step in MF-ROMP is under thermodynamic control. Notably, the value of $\psi$ increased with decreasing reaction temperature, indicating a better selectivity at low temperature, as expected (Figure 1c and Figure S2). Additionally, the *trans*/*cis* ratio was constant throughout the polymerization (Figure S3), which is consistent with both a thermodynamically controlled reaction where the last alkene can isomerize, as well as, a kinetically controlled process.

The interesting stereoselectivity warranted a deeper understanding of the mechanism of MF-ROMP. In contrast with our previously proposed cyclobutane radical cationic intermediate, a revised stepwise mechanism is proposed here (Figure 2).[26] In the revised mechanistic hypothesis, one electron oxidation of the enol ether generates the enol ether radical cation, which subsequently reacts with norbornene to form intermediate **i1**. Radical rearrangement in **i1** through a four-coordinate transition state (**TS1**) produces intermediate **i2**. Finally, ring opening of the bicycle via **TS2** results in the formation of **i3**, setting the stereochemistry of the backbone olefin. The proposed reaction paths from each diastereomer of **i1** to **i3**, resulting in either *trans* or *cis* products, are shown in Figure S5.

To understand which step determines the stereoselectivity, quantum chemical calculations were performed at the unrestricted B3LYP level of theory[40] and the 6-31G* basis set,[41] using the Growing String Method (GSM)[41,42] to simulate the reaction pathways for isomerization of **i2** and ring opening of **i3**. See the Supporting Information for full computational details. In our calculations, we used an isopropyl group to represent a simplified model for the polymer. The SMD solvation model was employed using dichloromethane and toluene as solvents.[44] Counteranion binding around the active chain end was neglected at this stage. The simulated activation barriers for the forward and reverse reactions from **i2** to **i3**, as well as the isomerization between all four diastereomers of **i2**, were each found to be less than 13.1 kcal mol$^{-1}$ in dichloromethane (Figure S6) and 14.5 kcal mol$^{-1}$ in toluene (Figure S7). These calculations suggest that

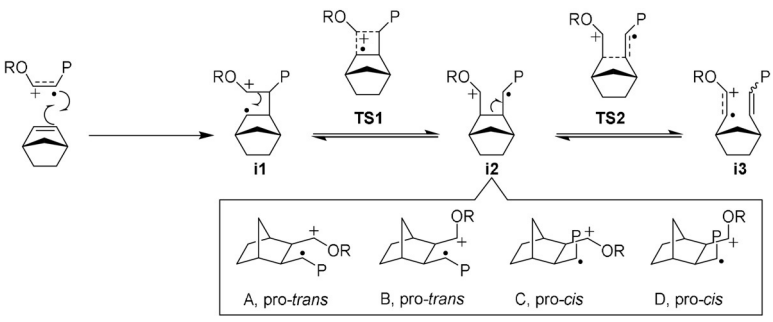


***Figure 2.*** Proposed mechanism of MF-ROMP, electron transfer and back electron transfer with **i3** are omitted; (inset) four diastereomers of **i2** and their pro-stereoisomerism.

  

rapid exchange may occur between the eight structures arising from **i2** and **i3**, and that the stereo-determining step is likely under thermodynamic control. Therefore, the relative ground state energies of isomers **A-D** of **i3** would determine the *trans*/*cis* ratio during MF-ROMP. Intuitively, it seemed unlikely that the reverse step from **i3** to **i2** would occur readily, since it constitutes reforming the strained [2.2.1] bicycle. This finding is consistent, however, with a previous study by Moeller and co-workers that found cyclization of an enol ether radical cation forms a [2.2.1] bicycle, which supports feasibility of our hypothesis.[45]

Next, **i3** diastereomers with ethyl groups showing *trans* (**i3-A** and **i3-B**) and *cis* (**i3-C** and **i3-D**) geometries with counteranion binding ($BF_4^-$ and $BAr^F{}_4^-$) were simulated (Figure 3). These calculations most closely resemble low temperature conditions. Gibbs free energies are reported relative to **i3-A** in each case. Absent a counteranion in dichloromethane solvent, **i3-A** and **i3-B** were found to be more stable than **i3-C** and **i3-D**. When incorporating $BF_4^-$ as the counteranion, **i3-B** was further stabilized whereas **i3-C** and **i3-D** were destabilized, indicating a scenario favoring *trans* alkene formation. **i3-B** is stabilized relative to **i3-A** and **i3-D** is stabilized relative to **i3-C** due to the ability of the counteranion to coordinate more closely to the radical cation when the active chain end is less sterically inhibited. Distances for charge separation are reported in Figure 3. The resultant difference in energy between **i3-B** and **i3-D** (the lowest energy *trans* and *cis* structures, respectively) leads to *trans* selectivity. This is consistent with the *trans*-dominant stereoselectivity observed experimentally. On the contrary, with $BAr^F{}_4^-$ as the counteranion in dichloromethane, **i3-B** was destabilized while **i3-C** and **i3-D** were stabilized with **i3-C** showing the lowest energy among the intermediates. Here, the *trans* products are destabilized because the growing polymer chain sterically inhibits the large $BAr^F{}_4^-$ anion from coordinating closely to the radical cation. Since the energies of **i3-A** and **i3-C** (0 and $-0.5$ kcal mol$^{-1}$, respectively) are within the error range of DFT calculations, it could explain why an almost 1:1 stereoselectivity was observed by using **2b** and **3c** in dichloromethane throughout the temperature window (Table 1, entries 3 and 4).

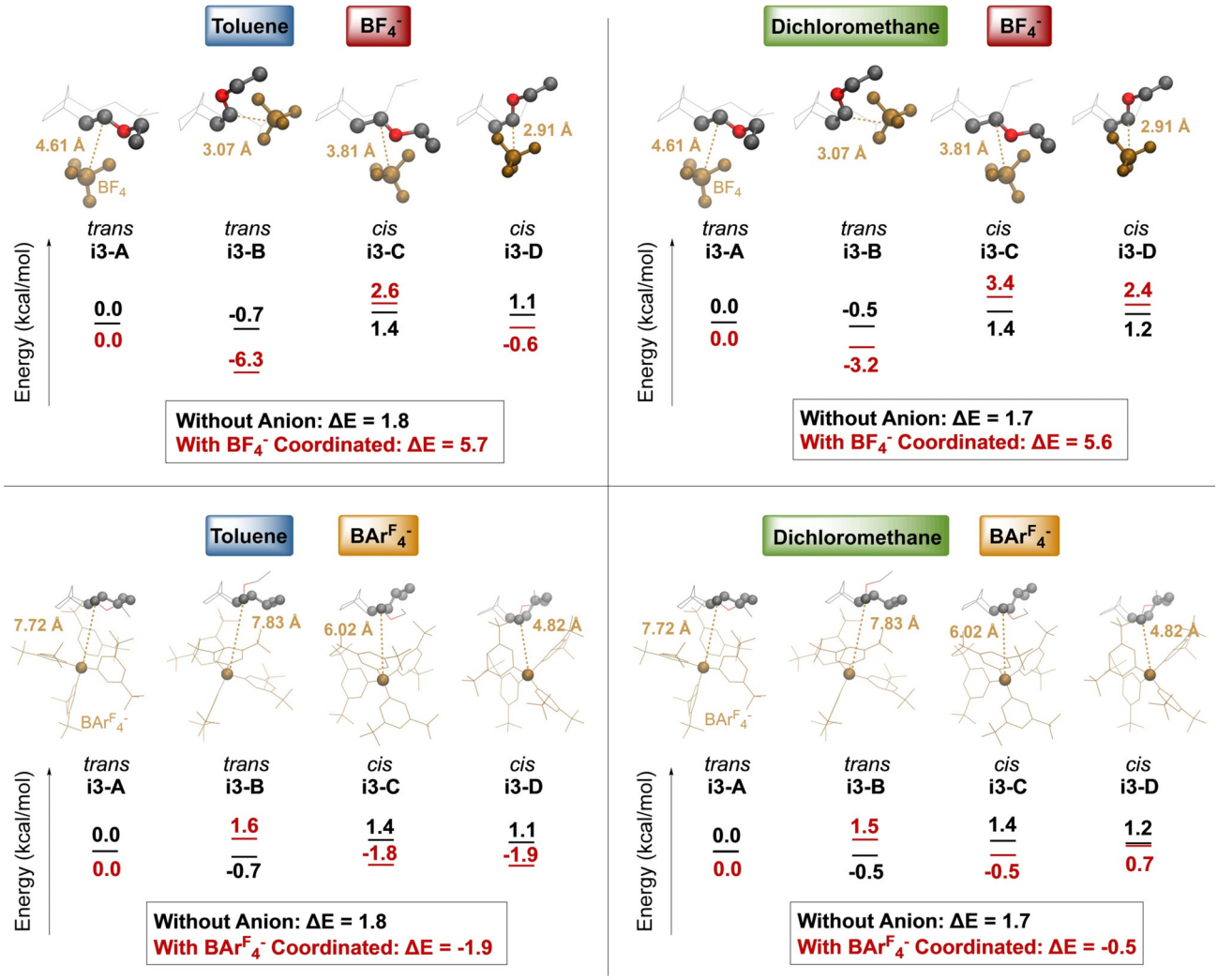


***Figure 3.*** The calculated structures of **i3** with each variant combination: dichloromethane (green) and toluene (blue) as solvents, $BF_4^-$ (red) and $BAr^F{}_4^-$ (orange) as counteranions. The $\Delta E$ reported for each data set corresponds to the difference in energy between the lowest energy *trans* structure and the lowest energy *cis* structure.

Switching the solvent from dichloromethane to toluene with no counteranions showed that *trans* products **i3-A** and **i3-B** are each lower in energy than their *cis* counterparts. The selectivity was completely reversed by introducing $BAr^{F}_{4}{}^{-}$ counteranion binding, where *cis* isomers **i3-C** and **i3-D** are each selectively stabilized and lower in energy than **i3-A** and **i3-B**. Although introducing $BAr^{F}_{4}{}^{-}$ into the model with either solvent leads to a *cis* preference, the stabilization in toluene was observed to be greater than in dichloromethane ($\Delta E = -1.9$ kcal mol$^{-1}$ in toluene and $-0.5$ kcal mol$^{-1}$ in dichloromethane) and therefore greater *cis* selectivity is observed in toluene. The computational results are in accord with the *cis* dominant selectivity observed experimentally using **2b** and **3c** in toluene at −76 °C (Table 1, entry 6). The drastic change in which isomer is stabilized is caused by a switch in the dominant steric interaction. Using $BF_4^-$, the dominant steric interaction is between the counteranion and radical cation, whereas when using $BAr^{F}_{4}{}^{-}$, the dominant steric interaction is between the counteranion and the growing polymer chain (Figure 3).

Overall, this model suggests that steric interactions between the active chain end and the photocatalyst counteranion, as well as solvation, play a critical role in determining the stereochemistry of MF-ROMP polymers. The computational results are consistent with the experimental findings that each set of reaction conditions examined using $BF_4^-$ as the counteranion resulted in a *trans* predominant reaction. Additionally, our data explains why *cis* alkene selectivity could astonishingly be achieved as a thermodynamically favored product using $BAr^{F}_{4}{}^{-}$ salts in toluene at low temperature. The calculations also support the *trans* dominant selectivity under all conditions using dichloromethane, because (1) even with the $BAr^{F}_{4}{}^{-}$ counteranion in dichloromethane the energy difference of *cis* and *trans* isomers is within DFT error; (2) higher temperature will permit more conformations of **i3** to be accessible, thus eroding the selective stabilization observed computationally; and (3) solvation of the radical cationic chain end by a polar solvent (dichloromethane) is more competitive than a noncoordinating bulky counteranion, thus diminishing the anion's ability to impact stereocontrol. This model also points toward the experimentally observed trends with varied initiator steric parameters. We would expect that as the steric bulk of the active chain-end increases, the counteranion would have weaker binding to the growing polymer. Species with tighter ion pairs experience more stabilization than ones with looser ion pairs. Therefore, sterically larger enol ethers, which inhibit tight ion binding, experience less selective stabilization from anion binding, and are more similar to the hypothetical anion-free scenario. This effect causes the *cis* structures to be more greatly destabilized relative to the *trans* structures as the R group on the active chain end increases in size. This trend can be observed in the data reported in Table S5.

## Conclusion

We report the first method for metal-free stereocontrol in ROMP, which was manifested largely from non-covalent interactions. By straightforward modification of reaction conditions, photocatalyst, and initiator structure, we were able to achieve 75 % *cis* olefins and > 98 % *trans* olefins in the backbone of polynorbornene. DFT calculations suggest the stereocontrolling step is likely under thermodynamic control. Additionally, the simulated models are consistent with experimentally observed stereoselectivity from counteranions, initiators, and solvent effects, collectively providing a basis for generalization and design parameters moving forward. This study demonstrates a new way of achieving stereocontrol in ROMP that leverages a metal free approach, is easily modifiable, avoids intricate catalyst or monomer designs, enriches our mechanistic understanding of photoredox MF-ROMP, and may provide new opportunities for the industrial production of precision ROMP products with tailored physicochemical properties.

## Acknowledgements

We thank Dr. Daniel Seidenkranz for suggesting that we investigate enol ether steric effects. The following instrumentation in the Paul Bender Chemical Instrumentation Center was sup-ported by: Bruker AVANCE 400 NMR spectrometer by NSF CHE-1048642; Bruker AVANCE 500 NMR spectrometer by a generous gift from Paul J. and Margaret M. Bender; Bruker AVANCE 600 NMR by NIH S10 OD012245; Thermo Q Exactive Plus by NIH 1S10 OD020022-1. We gratefully acknowledge financial support from the Army Research Labs (Cooperative Agreement No. W911NF-17-2-0199), the National Science Foundation (DMR-1452726 and CHE-2002886; CHE-1551994 to AGR and PMZ). AJB acknowledges partial financial support from the Yamamoto Family, the Office of the Vice Chancellor for Research and Graduate Education at the University of Wisconsin—Madison with funding from the Wisconsin Alumni Research Foundation.

## Conflict of interest

AJ Boydston has an equity part ownership of a company that has licensed technology related to that described in the manuscript.

**Stichwörter:** ion-pairing · metal-free · photoredox catalysis · ring-opening metathesis polymerization · stereoselectivity

[1] O. Nuyken, S. D. Pask, *Polymer* **2013**, *5*, 361 – 403.
[2] C. W. Bielawski, R. H. Grubbs, *Prog. Polym. Sci.* **2007**, *32*, 1 – 29.
[3] J. P. Bishop, R. A. Register, *JJ. Polym. Sci. B* **2011**, *49*, 68 – 79.
[4] T. Steinhäusler, W. J. Koros, *J. Polym. Sci. B* **1997**, *35*, 91 – 99.
[5] E. Rojo, M. E. Muñoz, A. Santamaría, B. Peña, *Macromol. Rapid Commun.* **2004**, *25*, 1314 – 1318.
[6] C. Agatemor, M. P. Shaver, *Biomacromolecules* **2013**, *14*, 699 – 708.
[7] T. D. Jones, K. A. Chaffin, F. S. Bates, B. K. Annis, E. W. Hagaman, M. Kim, G. D. Wignall, W. Fan, R. Waymouth, *Macromolecules* **2002**, *35*, 5061 – 5068.

  

[8] S. Hayano, Y. Nakama, *Macromolecules* **2014**, *47*, 7797 – 7811.
[9] G. C. Bazan, E. Khosarvi, R. R. Schrock, W. J. Feast, V. C. Gibson, M. B. O'Reagan, J. K. Thomas, W. M. Davis, *J. Am. Chem. Soc.* **1990**, *112*, 8378 – 8387.
[10] M. A. Esteruelas, F. González, J. Herrero, P. Lucio, *Polym. Bull.* **2007**, *58*, 923 – 931.
[11] R. O. Dell, D. H. Mcconville, G. E. Hofmeister, R. R. Schrock, *J. Am. Chem. Soc.* **1994**, *116*, 3414 – 3423.
[12] R. R. Schrock, J. Lee, R. O. Dell, J. H. Oskam, *Macromolecules* **1995**, *28*, 5933 – 5940.
[13] R. R. Schrock, A. H. Hoveyda, *Angew. Chem. Int. Ed.* **2003**, *42*, 4592 – 4633; *Angew. Chem.* **2003**, *115*, 4740 – 4782.
[14] M. M. Flook, V. W. L. Ng, R. R. Schrock, *J. Am. Chem. Soc.* **2011**, *133*, 1784 – 1786.
[15] M. M. Flook, J. Borner, S. M. Kilyanek, L. C. H. Gerber, R. R. Schrock, *Organometallics* **2012**, *31*, 6231 – 6243.
[16] R. R. Schrock, *Acc. Chem. Res.* **2014**, *47*, 2457 – 2466.
[17] L. Delaude, A. Demonceau, A. F. Noels, *Macromolecules* **2003**, *36*, 1446 – 1456.
[18] L. H. Peeck, S. Leuthäusser, H. Plenio, *Organometallics* **2010**, *29*, 4339 – 4345.
[19] B. K. Keitz, A. Fedorov, R. H. Grubbs, *J. Am. Chem. Soc.* **2012**, *134*, 2040 – 2043.
[20] L. E. Rosebrugh, V. M. Marx, B. K. Keitz, R. H. Grubbs, *J. Am. Chem. Soc.* **2013**, *135*, 10032 – 10035.
[21] L. E. Rosebrugh, T. S. Ahmed, V. M. Marx, J. Hartung, P. Liu, K. N. Houk, R. H. Grubbs, *J. Am. Chem. Soc.* **2016**, *138*, 1394 – 1405.
[22] Z. You, D. Gao, O. Jin, X. He, M. Xie, *J. Polym. Sci. A* **2013**, *51*, 1292 – 1301.
[23] H.-C. Yang, S.-Y. Lin, H.-C. Yang, C.-L. Lin, L. Tsai, S.-L. Huang, I. W.-P. Chen, C. Chen, B.-Y. Jin, T.-Y. Luh, *Angew. Chem. Int. Ed.* **2006**, *45*, 726 – 730; *Angew. Chem.* **2006**, *118*, 740 – 744.
[24] J. Peng, B. Panda, K. Satyanarayana, H. Yang, S. Huang, M. J. Huang, C. Chen, G. Lai, Y. Lai, T. Luh, *Macromolecules* **2019**, *52*, 7749 – 7755.
[25] A. E. Goetz, L. M. M. Pascual, D. G. Dunford, K. A. Ogawa, D. B. Knorr, A. J. Boydston, *ACS Macro Lett.* **2016**, *5*, 579 – 582.
[26] K. A. Ogawa, A. E. Goetz, A. J. Boydston, *J. Am. Chem. Soc.* **2015**, *137*, 1400 – 1403.
[27] A. J. Teator, F. A. Leibfarth, *Science* **2019**, *363*, 1439 – 1443.
[28] A. J. Teator, T. P. Varner, P. E. Jacky, K. A. Sheyko, F. A. Leibfarth, *ACS Macro Lett.* **2019**, *8*, 1559 – 1563.
[29] P. D. Morse, T. M. Nguyen, C. L. Cruz, D. A. Nicewicz, *Tetrahedron* **2018**, *74*, 3266 – 3272.
[30] Z. Yang, H. Li, S. Li, M. T. Zhang, S. Luo, *Org. Chem. Front.* **2017**, *4*, 1037 – 1041.
[31] K. Brak, E. N. Jacobsen, *Angew. Chem. Int. Ed.* **2013**, *52*, 534 – 561; *Angew. Chem.* **2013**, *125*, 558 – 588.
[32] X. Cui, K. Burgess, *Chem. Rev.* **2005**, *105*, 3272 – 3296.
[33] A. Brändström, *Adv. Phys. Org. Chem.* **1977**, *15*, 267 – 330.
[34] S. E. Denmark, N. D. Gould, L. M. Wolf, *J. Org. Chem.* **2011**, *76*, 4260 – 4336.
[35] H. Iwamoto, M. Yoshimura, T. Sonoda, H. Kobayashi, *Bull. Chem. Soc. Jpn.* **1983**, *56*, 796 – 801.
[36] S. Alvarez, *Chem. Eur. J.* **2020**, *26*, 4350 – 4377.
[37] F. Cataldo, *Eur. Chem. Bull.* **2015**, *4*, 92 – 97.
[38] M. S. Sigman, J. J. Miller, *J. Org. Chem.* **2009**, *74*, 7633 – 7643.
[39] L. You, J. S. Berman, A. Lucksanawichien, E. V. Anslyn, *J. Am. Chem. Soc.* **2012**, *134*, 7126 – 7134.
[40] A. D. Becke, *J. Chem. Phys.* **1993**, *98*, 1372 – 1377.
[41] V. A. Rassolov, J. A. Pople, M. A. Ratner, T. L. Windus, *J. Chem. Phys.* **1998**, *109*, 1223 – 1229.
[42] P. Zimmerman, *J. Chem. Theory Comput.* **2013**, *9*, 3043 – 3050.
[43] P. M. Zimmerman, *J. Chem. Phys.* **2013**, *138*, 184102.
[44] A. V. Marenich, C. J. Cramer, D. G. Truhlar, *J. Phys. Chem. B* **2009**, *113*, 6378 – 6396.
[45] S. H. K. Reddy, K. D. Moeller, *Tetrahedron Lett.* **1998**, *39*, 8027 – 8030.

Manuskript erhalten: 9. Dezember 2020
Veränderte Fassung erhalten: 25. Februar 2021
Akzeptierte Fassung online: 15. März 2021
Endgültige Fassung online: 7. Mai 2021

  